

Theoretical Studies of the Vibrational Spectra and Molecular Structures of Dosulepin and Doxepin

F. Shojaie

Department of Photonic, Institute of Science and High Technology and Environmental Sciences, Graduate University of Advanced Technology, P.O. Box: 76315-117, Kerman, Iran

(Received 21 November 2015, Accepted 26 March 2016)

Dosulepin and doxepin are tricyclic antidepressants. The molecular geometries, harmonic vibrational frequencies, quantum chemical parameters and thermodynamic properties of dosulepin and doxepin were calculated by Generalized Gradient Approximation methods developed by Perdew and Wang (GGA-PW91) and Becke-Lee-Yang-Parr (GGA-BLYP) in the gas phase and solution media. The local reactivity of these drugs was studied by the Fukui indices in order to predict both the reactive centers and the possible sites of nucleophilic and electrophilic attacks. Computational and chemical simulations were carried out for these drugs. Quantum chemical parameters of dosulepin and doxepin were calculated and compared. The simulation results show that dosulepin is quite a reactive drug. The fundamental modes of the vibrational frequencies were determined for dosulepin and doxepin. The BLYP/PW91 analyses of the wavenumbers show that the frequencies assigned to doxepin are higher than those assigned to dosulepin in the gas phase and solution media.

Keywords: Dosulepin, Doxepin, Infrared (IR) spectra, Quantum chemical parameters

INTRODUCTION

Dosulepin (formerly known as dothiepin) [3-dibenzo (b,e) thiepin-11(6H)-ylidene-N,N-dimethyl-1-propamine] and doxepin [3-dibenzo (b,e) oxepin-(6H)-ylidene-N,N-dimethyl-1-propanamine] are tricyclic antidepressant (TCAs). They have a tertiary amine chemical structure and have been used for the treatment of depression and anxiety disorders [1]. They have identical chemical structures except in the center ring where dosulepin has a sulfur atom, whereas doxepin has an oxygen atom.

The synthesis of dosulepin hydrochloride and doxepin hydrochloride by Grignard Reactions in Toluene was reported by Jalander, L [2]. Abdellatef *et al.* have proposed that spectrophotometric and spectrofluorimetric methods could be used for determination of tramadol, acebutolol and dosulepin hydrochlorides in pure forms and pharmaceutical formulations [3]. The absorption and fluorescence spectra of

dosulepin and doxepin in solvents with different polarities and in β -cyclodextrin have been recorded by Sankaranarayanan *et al.* [4]. They analyzed the solid inclusion complexes of both drugs by Fourier Transform Infrared (FT-IR) spectra and demonstrated that the absorption and emission maxima of dosulepin in solvents are redder shifted than doxepin. The reason that we have carried out this work is because we have not found any reports on structural studies of dosulepin and doxepin. The understanding of chemical and biological properties of compounds depends largely on knowledge of their molecular structures and spectral behaviors. This work describes the structural and vibrational properties of the dosulepin and doxepin. The purpose of this work is a detailed investigation of the vibrational spectra of dosulepin and doxepin.

Computational Details

Electronic and geometric structures of the dosulepin and doxepin molecules were calculated by the Dmol³ program

*Corresponding author. E-mail: f.shojaie@kgut.ac.ir

package in Materials Studio 5.5 [5-8]. The main calculations presented in this work are based on the Generalized Gradient Corrections (GGA) method developed by Perdew and Wang (PW91) and Becke-Lee-Yang-Parr (BLYP) [8-11]. The atomic orbital basis set was derived numerically for an atom in a centered grid using Double Numeric plus Polarization (DNP) functions. The size of the DNP basis set is comparable to 6-31G** Gaussian basis sets but more accurate. Total energy convergence criteria for Self-Consistent Field (SCF) were set to 10^{-6} eV. To improve computational performance in terms of fast SCF convergence, a smearing of 0.005 Hartree was considered.

Full geometry optimization was performed by examining species in the gas phase and solution media. The effect of the solvent in water was estimated by the Conductor-like Screening Model (COSMO) [12]. The dielectric constant of water was taken as 78.54 in this model. The drug conformers were considered to be minima based on the absence of imaginary frequencies, which provides a true minimum on the potential surface.

RESULTS AND DISCUSSION

Geometric Structure

The structures and the optimized configurations of dosulepin and doxepin are presented in Fig. 1. Table 1 shows the bond lengths and the bond angles of these drugs in accordance with the atom numbering schemes of the molecules as presented in Fig. 1. According to our calculations, the bond lengths and the bond angles of these two drugs in their gas phase are approximately equal to their corresponding bond lengths and bond angles in their solution media. The doxepin C5-O-C8 bond angle is wider than dosulepin C5-S-C8 bond angle in the gas phase and solution media and this is undoubtedly due to the higher steric repulsion caused by the shorter C5-O and C8-O bonds than C5-S and C8-S bonds, respectively [13]. The O-C8-C9 and O-C5-C4 bond angles are respectively greater than S-C8-C9 and S-C5-C4 in both phases. The differences between the doxepin O-C8-C9 and O-C5-C4 bond angles in the gas phase and their corresponding values in solution media (0.346, 0.368 degrees) are greater than the differences between dosulepin S-C8-C9 and S-C5-C4 bond angles in gas phase and their corresponding values in

solution media (0.076, 0.062). A possible explanation for this phenomenon is that the solvent has more influence on the polarization of oxygen atom than the sulfur atom.

IR Spectra

The dosulepin and doxepin molecules consist of 42 atoms, with 120 normal modes of fundamental vibrations. All of the normal modes are active in IR absorption in the gas phase and solution media. The calculated wavenumbers and assignments are given in Table 2.

CH₃ vibrations. Two methyl groups are present in dosulepin and doxepin which are directly connected to the nitrogen atom. For methyl groups, the asymmetric stretching vibrations are observed in the region 2950-3080 cm^{-1} and the symmetric stretching appears in the region 2900-2970 cm^{-1} [14]. For the two methyl groups of dosulepin, asymmetric stretching bands, calculated by the BLYP/PW91 method, occur in the regions 3001-3013 cm^{-1} and 3047-3048 cm^{-1} in the gas phase and in the regions 3011-3015 cm^{-1} and 3041-3047 cm^{-1} in solution media. For this compound, the symmetric stretching observed bands, calculated by BLYP/PW91 method, occur in the ranges 2837-2969 cm^{-1} and 2853-2999 cm^{-1} in the gas phase and in the ranges 2852-2966 cm^{-1} and 2867-2991 cm^{-1} in solution media.

The BLYP/PW91 calculations assign the ranges of asymmetric stretching vibrations of the methyl groups of doxepin to be 3017-3065 cm^{-1} and 3044-3100 cm^{-1} in the gas phase and 3013-3067 cm^{-1} and 3029-3103 cm^{-1} in solution media. The BLYP calculations assign values of symmetric stretching bands to be 2865, 2850 and 2836 cm^{-1} in the gas phase and 2860, 2864 and 2872 cm^{-1} in solution media. However, the PW91 method assigns values of symmetric stretching bands to be 2884, 2872 and 2853 cm^{-1} in the gas phase and 2894, 2887 and 2861 cm^{-1} in solution media.

The asymmetrical and symmetrical deformations are expected in the range 1400-1485 cm^{-1} and $1380 \pm 25 \text{ cm}^{-1}$ [14]. BLYP method calculates the ranges of the asymmetric stretching bands of dosulepin methyl group to be 1445-1492 cm^{-1} and 1441-1486 cm^{-1} in the gas phase and solution media respectively, and same ranges calculated by PW91 are 1436-1479 cm^{-1} and 1426-1474 cm^{-1} . For this compound, BLYP/PW91 calculations assign the asymmetric

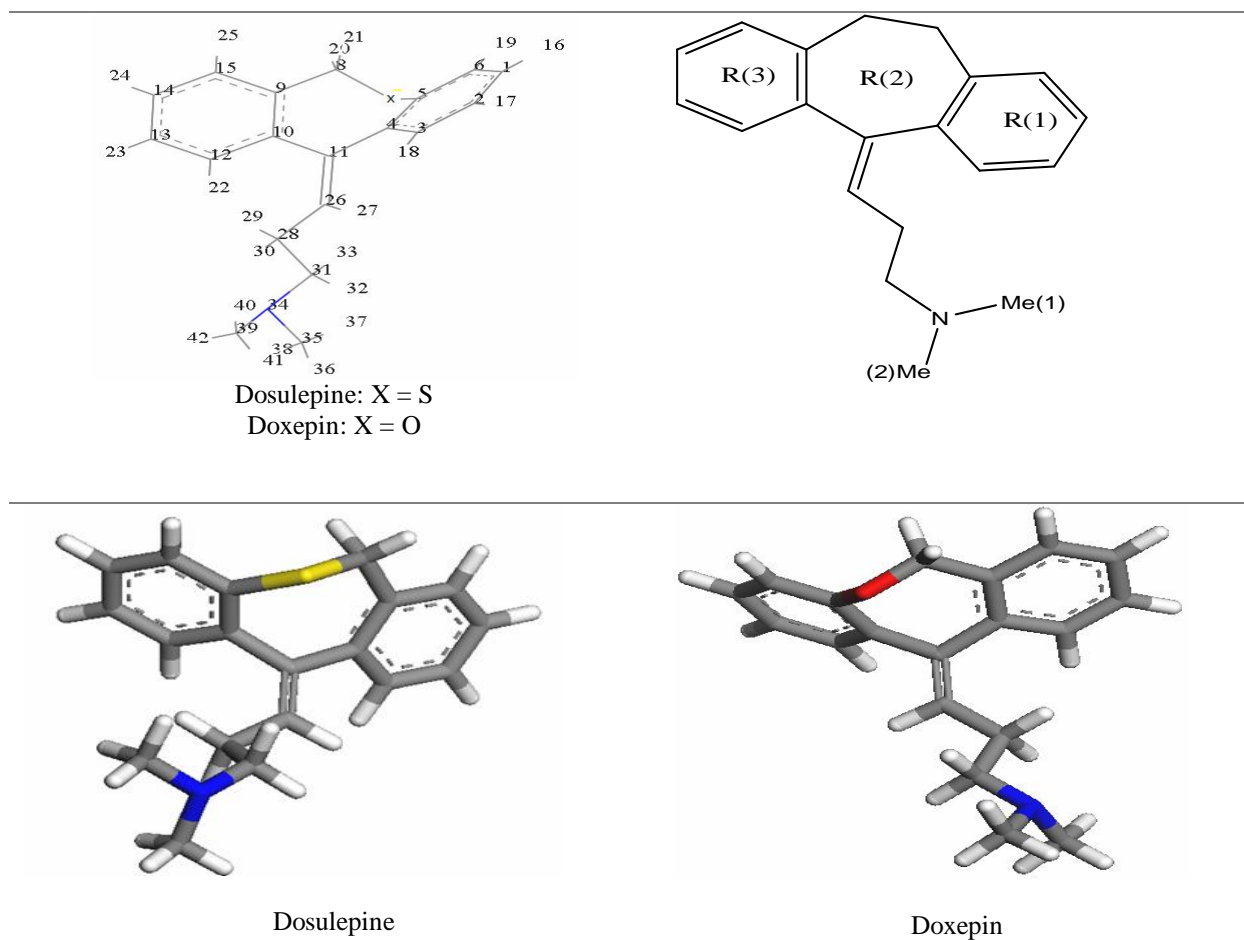


Fig. 1. The structures and the Optimized geometries (BLYP) of dosulepin and doxepin.

deformation band regions to be $1412\text{--}1432\text{ cm}^{-1}$ and $1402\text{--}1434\text{ cm}^{-1}$ in the gas phase and solution media respectively, and values of asymmetric deformation bands to be 1407 , 1427 and 1443 cm^{-1} in the gas phase and 1390 , 1430 and 1405 cm^{-1} in solution media.

The doxepin asymmetrical deformation modes have been determined in the ranges $1443\text{--}1491\text{ cm}^{-1}$ (BLYP) and $1446\text{--}1482\text{ cm}^{-1}$ (PW91) for gas phase and in the ranges $1442\text{--}1478\text{ cm}^{-1}$ (BLYP) and $1442\text{--}1482\text{ cm}^{-1}$ (PW91) for solution media. For this molecule, the BLYP/PW91 calculated values of symmetric deformation modes are 1416 cm^{-1} and 1433 , 1432 and 1402 cm^{-1} in the gas phase and 1408 , 1432 cm^{-1} and 1400 , 1426 and 1420 cm^{-1} in solution media. The regions of calculated frequencies for the methyl

groups of doxepin are similar to dosulepin in the gas phase and solution media.

Ring vibrations. The C-H stretching vibrations of aromatic structures generally occur in the region $3050\text{--}3150\text{ cm}^{-1}$. For the dosulepin, these modes have been calculated to be $3076\text{--}3127\text{ cm}^{-1}$ and $3097\text{--}3128\text{ cm}^{-1}$ by BLYP method and $3098\text{--}3141\text{ cm}^{-1}$ and $3096\text{--}3142\text{ cm}^{-1}$ by PW91 method in the gas phase and solution media, respectively. The regions of C-H stretching vibrations of the R1 and R3 rings of doxepin have been assigned to be $3102\text{--}3150\text{ cm}^{-1}$ by BLYP method and $3137\text{--}3182\text{ cm}^{-1}$ by PW91 method in the gas phase and same regions have been assigned to be $3122\text{--}3152\text{ cm}^{-1}$ by BLYP method and $3147\text{--}3184\text{ cm}^{-1}$ by PW91 method in solution media.

Table 1. Bond Lengths and Bond Angles of Dosulepin and Doxepin Optimized by BLYP and PW91

Bond lengths (Å)	Dosulepin				Doxepin			
	Gas		Solvent		Gas		Solvent	
Bond angles (degree)	BLYP	PW91	BLYP	PW91	BLYP	PW91	BLYP	PW91
C1-C2	1.401	1.397	1.402	1.398	1.400	1.396	1.401	1.397
C2-C3	1.401	1.397	1.402	1.398	1.401	1.396	1.402	1.397
C3-C4	1.408	1.403	1.409	1.404	1.406	1.401	1.408	1.402
C4-C5	1.412	1.407	1.412	1.407	1.408	1.403	1.408	1.404
C5-C6	1.404	1.400	1.405	1.400	1.398	1.393	1.398	1.393
C1-C6	1.400	1.396	1.401	1.397	1.401	1.396	1.402	1.397
C6-H19	1.088	1.089	1.089	1.090	1.088	1.089	1.089	1.089
C1-H16	1.089	1.057	1.089	1.090	1.089	1.089	1.089	1.089
C2-H17	1.089	1.090	1.089	1.090	1.089	1.089	1.089	1.089
C3-H18	1.089	1.090	1.089	1.090	1.089	1.090	1.089	1.090
C5-O	-	-	-	-	1.398	1.386	1.401	1.389
C5-S	1.804	1.786	1.806	1.787	-	-	-	-
C8-O	-	-	-	-	1.445	1.430	1.452	1.437
C8-S	1.858	1.836	1.858	1.836	-	-	-	-
C8-C9	1.525	1.514	1.525	1.514	1.528	1.516	1.527	1.515
C9-C10	1.420	1.415	1.422	1.416	1.417	1.412	1.419	1.414
C10-C11	1.503	1.492	1.505	1.493	1.496	1.486	1.499	1.489
C4-C11	1.503	1.492	1.503	1.492	1.497	1.487	1.498	1.488
C8-H20	1.097	1.098	1.096	1.097	1.097	1.097	1.096	1.097
C8-H21	1.098	1.099	1.098	1.099	1.104	1.104	1.101	1.102
C10-C12	1.416	1.409	1.417	1.411	1.415	1.410	1.416	1.411
C12-C13	1.396	1.392	1.397	1.393	1.395	1.391	1.396	1.392
C13-C14	1.399	1.394	1.400	1.396	1.400	1.395	1.401	1.397
C14-C15	1.397	1.393	1.398	1.394	1.396	1.391	1.397	1.392
C9-C15	1.409	1.404	1.411	1.405	1.407	1.402	1.408	1.403
C15-H25	1.091	1.091	1.090	1.091	1.091	1.092	1.090	1.091
C14-H24	1.089	1.089	1.089	1.090	1.089	1.089	1.089	1.089
C13-H23	1.090	1.090	1.090	1.090	1.089	1.089	1.089	1.089

Table 1. Continued

C12-H22	1.088	1.089	1.088	1.090	1.088	1.089	1.033	1.088
C11-C26	1.356	1.354	1.357	1.359	1.355	1.324	1.356	1.354
C26-H27	1.093	1.094	1.093	1.094	1.093	1.094	1.093	1.094
C26-C28	1.504	1.493	1.504	1.493	1.508	1.497	1.508	1.497
C28-C31	1.568	1.556	1.566	1.555	1.548	1.536	1.546	1.535
C31-N	1.472	1.459	1.477	1.464	1.476	1.462	1.481	1.466
C35-N	1.467	1.455	1.473	1.460	1.471	1.458	1.476	1.463
C39-N	1.466	1.453	1.472	1.459	1.471	1.457	1.477	1.463
C5-O-C8	-	-	-	-	114.656	114.147	114.406	113.854
C5-C-S8	97.682	97.305	98.090	97.838	-	-	-	-
O-C8-C9	-	-	-	-	117.738	117.619	117.170	117.051
C-S8-C9	119.852	119.461	119.537	119.219	-	-	-	-
C4-C11-C10	120.004	120.334	120.005	120.309	117.442	117.806	117.085	117.445
O-C5-C4	-	-	-	-	119.167	119.274	118.821	118.906
C-S5-C4	119.170	118.864	119.094	118.802	-	-	-	-
C4-C11-C26	120.690	120.247	120.642	120.278	118.362	118.294	117.085	118.462
H20-C8-H21	106.995	106.728	107.052	106.728	107.491	107.296	107.546	107.259
C8-C9-C10	126.021	125.597	126.271	125.278	125.633	125.599	125.976	125.913
C31-N-C35	114.410	114.036	113.758	113.446	111.012	110.872	110.490	110.261
C31-N-C39	114.563	114.222	113.833	113.502	112.771	112.678	112.203	112.067
C35-N-C39	112.660	112.468	111.953	111.718	110.653	110.574	110.067	109.956

Table 2. Theoretical Vibrational Wavenumbers of Dosulepin and Doxepin

Assignments (cm ⁻¹)	Dosulepin				Doxepin			
	Gas		Solvent		Gas		Solvent	
	BLYP	PW91	BLYP	PW91	BLYP	PW91	BLYP	PW91
ν_s [R(1):(C-H)]	3127	3141	3128	3142	3150	3182	3152	3184
ν_s [R(3):(C-H)]	3121	3137	3124	3139	3148	3183	3147	3180
ν [R(3):(C-H)]	3110	3122	3110	3121	3135	3163	3139	3167
ν [R(1):(C-H)]	3111	3118	3112	3125	3134	3161	3138	3166
ν [R(3):(C-H)]	3101	3102	3105	3103	3127	3157	3132	3162

Table 2. Continued

ν [R(1):(C-H)]	3103	3107	3104	3106	3122	3150	3127	3153
ν [R(3):(C-H)]	3093	3098	3097	3096	3112	3138	3122	3147
ν_{as} [R(1):(C15-H25), (C14-H24)]	3076	3081	3080	3084	3102	3137	3114	3132
ν [(C26-H27), (C28-H30)]	3055	3070	3057	3067	3075	3101	3077	3095
ν [(C26-H27)] and ν_{as} [(H29-C28-H30), (H32-C31-H33)]	3029	3039	3031	3043	3049	3071	3039	3056
ν_{as} [Me(1):(H40-C39-H42), Me(2):(H36-C35-H37)]	3013	3048	3015	3047	-	-	-	-
ν_{as} [Me(1):(H40-C39-H42), Me(2):(H36-C35-H37)]	3001	3047	3011	3041	-	-	-	-
ν_{as} [Me(1):(H40-C39-H42)]	-	-	-	-	3065	3094	3067	3103
ν_{as} [Me(2):(H36-C35-H38)]	-	-	-	-	3059	3100	3059	3095
ν_{as} [R(2):(H20-C8-H21)]	3016	3027	3027	3037	3033	3047	3046	3055
ν_{as} [Me(2), Me(1), (H32-C31-H33)]	-	-	-	-	3017	3050	3013	3057
ν [(C31-H33), (C28-H29)] and ν_{as} [Me(1), Me(2)]	-	-	-	-	3027	3048	3016	3045
ν_{as} [(H33-C31-H33), Me(1), Me(2)] and ν_s [H29-C28-H30]	-	-	-	-	3025	3044	3026	3029
ν_{as} [(H32-C31-H33)] and ν [(H30-C28)]	3002	3013	2998	3003	-	-	-	-
ν_s [Me(1):(H40-C39-H42), Me(2):(H36-C35-H38)]	2969	2999	2966	2991	-	-	-	-
ν_s [Me(1):(H40-C39-H42), Me(2):(H36-C35-H38)]	2964	2997	2965	2989	-	-	-	-
ν_s [R(2):(H20-C8-H21)]	2962	2969	2972	2976	2948	2958	2969	2970
ν_s [(H32-C31-H33), (H30-C28-H29)]	2948	2965	2954	2965	2963	2976	2964	2975
ν [(C31-H32)] and ν_s [Me(1):(C39-H41), Me(2):(C35-H37)]	-	-	-	-	2865	2884	2872	2894
ν_s [(H32-C31-H33), (H29-C28-H30)]	2944	2958	2949	2952	-	-	-	-
ν_s [Me(1), Me(2)]	2847	2879	2866	2873	2850	2872	2864	2887
ν_s [Me(1), Me(2)] and ν_{as} [(H32-C31-H33)]	-	-	-	-	2836	2853	2860	2861
ν_s [Me(1), Me(2)]	2837	2853	2852	2867	-	-	-	-
ν_s [(C11-C26), (R(1):(C14-C15), (C10-C12)), (C26-C28)], δ [(C11-C26-H27), R(1), (H29-C28-H30)]	1595	1618	1591	1614	1613	1646	1616	1641
ν_s [(R(1):(C12-C13), (C14-C15), (R(3):(C2-C3), (C5-C6), (C11-C26), (R(2):(C4-C11), (C10-C11)], δ [R(1), R(2), R(3), (C11-C26-H27), (H29-C28-H30)]	1570	1603	1564	1598	1582	1607	1578	1601

Table 2. Continued

ν_s [(R(3):(C2-C3), (C5-C6), (R(1):(C13-C12), (C14-C15), (C11-C26)] and δ [R(1), R(2), R(3), (C11-C26-H27), (H29-C28-H30), (H20-C8-H21)]	1575	1596	1569	1592	1579	1603	1574	1599
ν_s [(R(3):(C1-C2), (C5-C4), (R(1):(C13-C14), (C9-C10), (C11-C26)] and δ [R(1), R(2), R(3), (C11-C26-H27)]	1555	1578	1546	1574	1556	1571	1551	1571
ν_s [(R(3):(C1-C2), (C5-C4)), (R(1):(C13-C14), (C9-C10), (C11-C26)] and δ [R(1), R(2), R(3), (C11-C26-H27), (H20-C8-H21)]	1549	1575	1544	1572	1550	1567	1541	1558
δ_{as} [Me(1), Me(2)] and δ_s [(H32-C31-H33), (H29-C28-H30)]	1492	1486	1479	1474	1491	1482	1478	1482
δ_{as} [Me(1), Me(2)] and δ_s [(H32-C31-H33), (H29-C28-H30)]	1475	1468	1470	1464	1482	1471	1476	1464
δ_{as} [Me(1), Me(2)] and δ_s [(H32-C31-H33), (H29-C28-H30)]	1472	-	-	-	1478	1464	1465	1450
δ_{as} [Me(1), Me(2)] and δ_s [(H32-C31-H33), (H29-C28-H30)]	-	-	-	-	1467	1450	1454	1436
ν_s [(R(1):(C14-C13), (C9-C10)], δ_s [(H20-C8-H21)] and δ [R(1)]	1468	1484	1465	1479	1479	1485	1470	-
γ [R(3), R(1)] and δ_s [(H20-C8-H21)]	1424	1406	1423	1388	1471	1478	1464	1468
δ_{as} [Me(1), Me(2), (H32-C31-H33), (H29-C28-H30), (H20-C8-H21)]	-	-	-	-	1460	1459	-	1455
δ_s [(H32-C31-H33), (H29-C28-H30), (H20-C8-H21), R(1), R(2), R(3)] and δ_{as} [Me(1), Me(2)]	1453	1465	1449	1466	1458	1457	1453	1449
δ_s [(H32-C31-H33), (H29-C28-H30), (C-N-C)] and δ_{as} [Me(1), Me(2)]	1460	1460	1461	1450	-	-	-	-
δ_s [(H32-C31-H33), (H29-C28-H30), (C-N-C)] and δ_{as} [Me(1), Me(2)]	1457	1444	1450	1442	1452	1446	1445	1442
δ_s [(H32-C31-H33), (H29-C28-H30)] and δ_{as} [Me(1), Me(2)]	1445	1441	1436	1426	1443	-	1442	-
δ_s [Me(2), Me(1), (H32-C31-H33), (H29-C28-H30), (C-N-C)]	1432	1415	1443	1405	-	-	1432	-
δ_s [(H20-C8-H21), Me(2), Me(1), (H32-C31-H33), (H29-C28-H30)] and γ [R(1),R(3)]	1431	1432	1427	1430	-	1432	-	1420
δ_s [(H20-C8-H21), Me(2), Me(1), (H32-C31-H33)] and γ [R(1)]	-	1434	-	1432	-	1433	-	1426

Table 2. Continued

δ_s [(H20-C8-H21)] and γ [R(1), R(3)]	1427	1426	1420	1423	1438	1436	1433	1430
δ_s [(H20-C8-H21)] and γ [R(1), R(3)]	-	-	1410	-	1431	-	1426	1422
δ_s [Me(1), Me(2)]	1412	1402	1407	1390	1416	1402	1408	1400
δ_s [(C11-C26-H27)] and γ [R(1), R(2), R(3)]					-	1356	-	1355
ω [(H32-C31-H33), (H29-C28-H30), (C11-C26-H27), (H20-C8-H21)], ν_s [(R(1):(C10-C12), (C13-C14), (C9-C15), (R(3):(C1-C2), (C3-C4), (C5-C6), (R(2):(C3-C9), (C4,C11)], and δ [R(1), R(2), R(3)]	-	1356	-	1354	-	1327	-	1332
ω [(H32-C31-H33), (H29-C28-H30), (H20-C8-H21), Me(1), Me(2)]	-	-	-	-	1375	1371	1384	1359
ω [(H32-C31-H33), (H29-C28-H30), (C11-C26-H27), (H20-C8-H21)] and δ [R(1), R(2), R(3)]	1309	1343	1305	1340	1370	1365	1371	1365
ω [(H32-C31-H33), (H29-C28-H30), (C11-C26-H27), (H20-C8-H21)] and δ [R(1), R(2), R(3)]	1354	-	1353	-	1361	-	1362	-
ω [(H32-C31-H33), (H29-C28-H30), (C11-C26-H27)]	1365	1335	1356	1335	-	-	-	-
γ [(H32-C31-H33), (H29-C28-H30)] and ω [(Me(1):(H41-C39-H41), (Me(2):(H36-C35-H37)]	1339	1328	1326	1329	1311	1309	1323	1306
δ_s [(C11-C26-H27)], ν_s [(R(1):(C10-C12), (C13-C14), (C9-C15), (R(3):(C1-C2), (C3-C4), (C5-C6), (R(2):(C3-C9), (C4,C11)], γ [(H32-C31-H33), (H29-C28-H30)] and δ [R(3)]	1293	1350	1289	1344	1300	1323	1298	1320
ω [(H29-C28-H30), R(1), R(2), R(3)] and γ [(H32-C31-H33), (C28-H29)]	1287	1286	1284	1284	1292	1294	1295	1288
δ_s [R(1)], ν_s [(C9-C10), ω [(H29-C28-H30), (H32-C31-H33)] and γ [R(3), (H21-C8-H20), (O-C)]	-	-	-	-	1289	-	1283	-
γ [(H20-C8-H21), R(3)] and ω [(C28-H30), (C26-H27)]	-	-	-	-	1276	1275	1275	1271
ω [(H20-C8-H21), (H29-C28-H30), (C11-C26-H27), (H32-C31-H33)], γ [R(1), R(3), Me(1), Me(2), (C-N)] and δ_s [(C-N-C), (C8-C9-C15)]	1262	1275	1254	1273	1274	1271	1271	1261
ω [(H20-C8-H21), (H29-C28-H30), (C11-C26-H27), (H32-C31-H33)], γ [R(1), R(3), Me(1), Me(2), (C-N)] and δ_s [(C8-C9-C15), (C-N-C)]	1272	1270	1270	1263	-	1263	-	1257

Table 2. Continued

γ [(H20-C8-H21), R(1), R(2), R(3)]	-	-	-	-	1264	-	1260	-
ω [(H32-C31-H33)] and γ [(H29-C28-H30)]	1248	1247	1247	1243	-	-	-	-
ω [(H32-C31-H33), (H29-C28-H30), (C26-H27), Me(1), Me(2)] and γ [R(3)]	1247	1242	1237	1247	-	-	-	-
ν_s [R(2):(C11-C10)], ω [(C11-C26-H27)] and γ [R(1), R(2), R(3), (H32-C31-H33), (H29-C28-H30), (N-C), Me(2)]	1230	1234	1230	1232	-	-	-	-
δ [(R(1), R(2), R(3)), γ [(C11-C26-H27), (C28-H29), (H32-C31-H33), Me(1), Me(2), (C-N)] and ν_s [R(2):(C4-C11), (C5-O)]	-	-	-	-	1219	1203	1217	1196
ω [(H32-C31-H33), (H30-C28-H29), (C26-H27), R(1), R(3), [(H21-C8-H20)] and ν_s [R(2):(C-O)]	-	-	-	-	1180	1237	1172	1232
γ [(H20-C8-H21), (H32-C31-H33), (H30-C28-H29), (C26-H27), R(1), R(2), R(3)]	1214	1167	1211	1162	1238	1260	1237	1250
ω [(H32-C31-H33), (H30-C28-H29), (C26-H27), (H21-C8-H20)] and γ [R(1), R(2), R(3)]	1154	1221	1155	1214	-	-	-	-
γ [(Me(1), Me(2), (C-N), (H32-C31-H33), (H30-C28-H29)]	-	-	-	-	1255	1221	1247	1220
δ_s [R(1), R(2)], ν_s [R(2):(C-O)] and ω [(H20-C8-H21)]	-	-	-	-	1169	1178	-	1176
δ_s [R(1):(H25-C15-C14-H24)] and γ [Me(1), Me(2), (C-N), (H32-C31-H33), (H30-C28-H29), (C26-H27)]	-	-	-	-	1163	1172	1161	1167
δ_s [R(1):(H25-C15-C14-H24)] and γ [Me(1), Me(2), (C-N), (H32-C31-H33), (H30-C28-H29), (C26-H27)]	-	-	-	-	-	-	1159	-
γ [(C11-C26-H27)] and δ [R(1)]	1186	1188	1182	1176	-	-	-	-
δ [(R(1), R(2), R(3)), γ [(C28-H29), (H32-C31-H33), Me(1), Me(2), (C-N), (H21-C8-H20)] and ω [(C26-H27)]	1147	1160	1141	1160	1160	1168	1153	1162
δ [(R(1), R(2), R(3)), γ [(C28-H29), (H32-C31-H33), Me(1), Me(2), (C-N), (H21-C8-H20)] and ω [(C26-H27)]	-	-	1148	-	-	-	-	-
γ [(H30-C28-H29), (H32-C31-H33), Me(1), Me(2), (C-N), (C26-H27)], δ_s [(C-N-C)] and ω [R(1), R(3)]	1153	1154	1151	1153	1145	1142	1140	1138
δ [R(1), R(3)]	-	-	-	-	1156	1158	1150	1146

Table 2. Continued

δ [R(1)]	1164	1153	-	1147	-	-	-	-
δ [R(3)]	1162	1149	1154	1141	-	1150	-	1139
δ [R(1), R(3), (H32-C31-H33), (H29-C28-H30), Me(1), Me(2), (N-C)] and ω [(C26-H27)]	1141	1146	1134	1143	1152	-	1145	-
δ [R(1)] and γ [Me(1), Me(2), (C-N), (H32-C31-H33), (H30-C28-H29), (C26-H27)]	-	-	-	-	1105	1110	1100	1106
δ [R(3)]	1113	1121	1110	1118	-	-	-	-
δ [(R(1), R(2), R(3))] and γ [Me(1), Me(2)]	1095	1103	1087	1099	1093	1101	1089	1099
γ [Me(1), Me(2), (C-N), R(3)] and ω [(H32-C31-H33), (H30-C28-H29), (C26-H27)]	1096	1099	1088	1091	1100	1052	1091	1042
γ [R(1), R(3), Me(1), Me(2), (H32-C31-H33), (H29-C28-H30), (N-C)] and ω [(C26-H27)] and ν [(N-C35), (N-C39)]	1073	1075	1070	1075	1083	1087	1080	1087
δ_s [R(1), R(3)] and γ [(H32-C31-H33), (H29-C28-H30), Me(1), Me(2), (C11-C26-H27)]	1048	1057	1045	1054	1044	1057	1037	1050
δ_s [R(1), R(3)] and γ [(H32-C31-H33), (H29-C28-H30), Me(1), Me(2), (C11-C26-H27)] and ω [(H20-C8-H21)]	1046	1048	1041	1048	-	1100	-	1092
ν [(N-C35)] and δ [Me(1), Me(2), (H32-C31-H33), (H30-C28-H29)]	1013	-	1004	-	1032	1032	1024	1027
δ_s [C39-N-C35], γ [Me(2), Me(1)] and ω [(C31-H33), (H29-C28-H30)] ν [(N-C31)]	1033	1036	1023	1023	-	-	-	-
δ_s [R(3)]	-	-	-	1039	-	-	-	-
γ [Me(2), Me(1)]	-	-	-	1034	-	-	-	-
δ_s [[R(3):(C-H)], γ [Me(2), Me(1)]	1027	1042	1025	-	1028	1035	1025	1028
δ_s [[R(3):(C-H)], γ [Me(2), Me(1)]	-	1041	-	-	-	-	-	-
ω [(H32-C31-H33), (H30-C28-H29)] and γ [Me(2), Me(1)]	-	-	-	-	1013	-	1008	-
γ [(C31-H33), (H29-C28-H30)], ω [(C26-H27)] and δ_s [H42-N-C36]	993	993	986	989	-	-	-	-
ω [R(3)]	974	974	986	980	-	-	-	-
ν [(C-O)], δ [R(1), R(2), R(3)], ω [(H32-C31-H33), (H30-C28-H29)] and γ [Me(2), Me(1)]	-	-	-	-	-	1022	-	1007
ω [(C31-H32), (C28-H29)], γ [(C11-C26-H27), Me(2), Me(1)] and ν [(N-C), (C28-C26)]	-	-	-	-	1003	1005	1001	1001

Table 2. Continued

ν_s [(O-C)], γ [Me(2), Me(1)] and ω [(H20-C8-H21), (H30-C28-H29), R(1), R(3)]	-	-	-	-	990	1023	971	1015
δ [H20-C8-H21]	-	-	-	-	1010	-	1006	-
ω [R(3)]	941	941	949	943	957	963	975	959
ω [R(1)]	962	929	963	964	-	966	-	971
ω [R(1), R(3), (H32-C31-H33), (H30-C28-H29)] and γ [(H20-C8-H21), (C11-C26-H27)]	929	959	934	960	-	-	-	-
γ [(Me(1), Me(2), (C-N)] and ω [(H32-C31-H33), (H30-C28-H29), (C11-C26-H27), R(1), R(2), R(3)], ν [(O-C)]	-	-	-	-	981	-	979	-
ω [R(1)] and γ [(H20-C8-H21)]	936	-	941	-	982	998	974	994
ω [R(1), R(3), (H32-C31-H33), (H30-C28-H29)] and γ [(H20-C8-H21), (C11-C26-H27)]	901	907	900	907	-	-	-	-
ω [R(3), R(1)] and γ [(H20-C8-H21)]	-	954	-	931	941	937	936	927
ω [R(1), R(3)] and γ [H32-C31-H33), (H30-C28-H29), (H20-C8-H21), (C11-C26-H27)]	872	879	874	877	-	-	-	-
ω [(R(1), R(3), R(2)), (H32-C31-H33)] and γ [(H30-C28-H29), (C11-C26-H27), (H20-C8-H21)]	890	868	889	867	902	912	901	907
ω [R(3), R(2), R(1)], γ [H30-C28-H29), (C26-H27)]	862	863	868	861	921	931	932	916
ν [(N-C35)], γ [(C11-C26-H27), (H30-C28-H29)] and ω [(H32-C31-H33)]	-	-	-	-	-	870	-	869
δ [(R(1), R(3)] and γ [(H20-C8-H21), (C11-C26-H27)]	-	-	-	-	865	-	864	-
ω [R(3),R(1)], γ [(H20-C8-H21) and δ [(C26-H27)]	-	836	-	835	-	-	-	-
ω [R(3), (H32-C31-H33), (H30-C28-H29)] and δ [(C26-H27)]	843	-	844	-	854	862	860	851
ν_s [(C35-N-C39-C31)]	803	818	799	809	-	-	-	-
δ [R(1), R(2), R(3)], ω [Me(1), Me(2), (H32-C31-H33), (H20-C8-H21)] and γ [H30-C28-H29), (C11-C26-H27)]	-	-	-	-	849	851	845	842
ω [R(3), R(1), (H32-C31-H33), (H30-C28-H29), (H20-C8-H21), (O-C)] and δ [(C26-H27)]	-	-	-	-	849	851	845	842
ω [(H32-C31-H33), (H20-C8-H21), (H30-C28-H29), Me(1), Me(2)], δ [R(1), R(2)] and γ [(C11-C26-H27)]	-	812	-	810	-	-	-	-

Table 2. Continued

ν_s [(C35-N-C39-C31)], ω [R(1), R(2), R(3), Me(1)] and γ [(H32-C31-H33), (H30-C28-H29), (C11-C26-H27)]	794	-	783	-	820	841	819	834
δ [R(1), R(2), R(3), Me(1), Me(2)] and γ [(H32-C31-H33), (H30-C28-H29), (C11-C26-H27), (C11-C26-H27)]	789	783	790	783	809	820	807	819
γ [(H29-C28-H30), (H32-C31-H33), (H20-C8-H21), (C-S)] and ω [R(3), R(1)]	765	755	766	759	-	-	-	-
γ [R(1), (H29-C28-H30), (H32-C31-H33), (H20-C8-H21), (C-O)] and ω [R(3)]	-	-	-	-	788	799	788	792
ω [R(3), R(1)]	748	748	753	747	-	-	-	-
δ [(H29-C28-H30), (H32-C31-H33)]	-	-	-	-	775	784	773	771
ω [R(1), R(2), R(3), (C11-C26-H27)] and γ [(H29-C28-H30), (H32-C31-H33)]	744	738	744	741	763	766	765	759
ω [R(1), R(3), (H20-C8-H21)]	714	718	717	718	750	756	756	746
ω [R(1), R(3)] and γ [(H32-C31-H33), (H30-C28-H29), (C26-C27)]	726	729	723	728	738	738	737	728
τ [R(1), R(2), R(3), (C11-C26-H27)] and γ [(H20-C8-H21)]	692	704	690	703	720	717	715	715
δ [R(1), R(2), R(3)] and γ [(C11-C26-H27), (C11-C26-H27)]	667	669	664	667	680	683	677	681
δ [R(1), R(3)], (H32-C31-H33), (H30-C28-H29), (C26-C27)] and γ [(C11-C26-H27)]	655	653	654	654	648	652	648	649
δ [R(3), R(1), R(3), (C11-C26-H27)] and γ [(H29-C28-H30), (H32-C31-H33)]	632	627	629	626	631	632	631	628
γ [R(3), R(1), (H20-C8-H21), (C11-C26-H27), (H29-C28-H30)]	592	594	592	593	590	594	590	591
γ [R(3), R(1), (H20-C8-H21), (C-O), (C11-C26-H27)]	-	-	-	-	662	624	620	621
ω [R(1), R(3), (C11-C26-H27), (H32-C31-H33), (H29-C28-H30), (H20-C8-H21)], δ_s [(H42-N-H36)], γ [(C-S), (H20-C8-H21)]	568	570	568	570	-	-	-	-
ν_s [(C-S)], δ_s [(H42-N-H36)], ω [R(1), R(3), (C11-C26-H27), (H32-C31-H33), (H29-C28-H30)], γ [(C-S), (H20-C8-H21)]	524	529	524	528	-	-	-	-
γ [R(3), R(1), (H20-C8-H21), (C-O), (C11-C26-H27)]	-	-	-	-	555	559	557	558
δ_s [(H42-N-H36)], ω [R(1), R(3), (C11-C26-H27), (H32-C31-H33), (H29-C28-H30)], γ [(C-S), (H20-C8-H21)]	506	511	508	511	-	-	-	-

Table 2. Continued

γ [R(3), R(1), (H29-C28-H30)] and ω [(H20-C8-H21), (C26-H27), (C-O)]	-	-	-	-	541	544	541	542
ω [R(1), R(3), (C11-C26-H27)] and γ [(H32-C31-H33), (H29-C28-H30), (H20-C8-H21), (C-S)]	485	489	487	488	-	-	-	-
γ [Me(1), Me(2), R(3), R(1), (H20-C8-H21), (N-C)] and ω [(H32-C31-H33), (H29-C28-H30), (C11-C26-H27), (C-O)]	-	-	-	-	505	507	507	509
ω [R(1), R(3)] and γ [(H20-C8-H21), (C-S), (C26-C27)]	452	455	455	452	-	-	-	-
δ [R(3), R(1), (H20-C8-H21), (C-O)]	-	-	-	-	474	476	471	470
τ [(C35-N-C39)], δ_s [(C31-N-C39)], γ [(H32-C31-H33), (H29-C28-H30), (H20-C8-H21), (C-S)] and ω [(R(1), R(3))]	446	449	778	448	-	-	-	-
γ [Me(1), Me(2), R(3), (H20-C8-H21), (C-O), (C-N)], ω [(H32-C31-H33), (H29-C28-H30), (C11-C26-H27)] and δ [(R(1), R(3))]	-	-	-	-	464	467	464	466
τ [(C35-N-C39)], δ_s [(C31-N-C39)] and γ [(H32-C31-H33)]	420	413	421	417	-	-	-	-
γ [R(3), R(1), (H20-C8-H21), (H32-C31-H33)] and ω [(C-O)]	-	-	-	-	451	450	450	446
δ [(C35-N-C39), ω [(H32-C31-H33), (H29-C28-H30), (C11-C26-H27), R(1), R(3)] and γ [(H20-C8-H21), (C-S)]	408	409	408	407	-	-	-	-
γ [Me(1), Me(2), (N-C)] and ω [(H32-C31-H33), (H29-C28-H30), R(3), R(1), (H20-C8-H21), (C11-C26-H27), (C-O)]	-	-	-	-	441	444	443	443
γ [Me(1), R(1), (H20-C8-H21)], τ [(H32-C31-H33), (H29-C28-H30)] and ω [(C11-C26-H27), R(2), R(3)]	388	392	388	393	-	-	-	-
γ [Me(2), (H32-C31-H33), (H29-C28-H30), (H20-C8-H21)], ω [(C26-27), Me(1), (N-C), R(1), R(3)] and ν [(C11-C26)]	-	-	-	-	425	426	423	424
γ [Me(1), Me(2), R(1), (H20-C8-H21)], ω [(C26-H27), (H32-C31-H33), (H29-C28-H30)] and τ [R(3)]	383	388	387	392	-	-	-	-
γ [Me(2), (H32-C31-H33)], ω [(C11-C26-H27), (H20-C8-H21), (N-C), Me(1)] and δ [(R(1), R(3))]	-	-	-	-	386	386	399	386
γ [Me(1), Me(2), (H32-C31-H33), R(3), (H20-C8-H21)] and ω [(C26-H27)]	373	378	373	376	376	375	378	376
γ [(C11-C26-H27), (N-C), Me(1), Me(2), (C-S)], τ [R(1), R(2)] and ω [(H29-C28-H30), (H32-C31-H33)]	330	335	332	337	-	-	-	-

Table 2. Continued

δ [(H32-N-H41)], γ [Me(1), Me(2), (H33-C31-H32), R(1), R(2), R(3)] and ω [(C11-C26-H27)]	-	-	-	-	359	362	363	363
γ [(H32-C31-H33), (H29-C28-H30), (C11-C26-H27)] and [(H29-C28-H30), (C-S), R(2), R(1)]	307	310	306	306	-	-	-	-
γ [(H32-C31-H33), (H29-C28-H30), (C11-C26-H27), R(3), R(1), R(3)] τ [Me(1), Me(2)]	-	-	-	-	323	328	322	324
ω [(H20-C8-H21), R(1), R(3), (C11-C26-H27), (H29-C28-H30), (C-S), (N-C)] and γ [CH ₃ (2), Me(1), (H32-C31-H33)]	286	286	286	287	-	-	-	-
τ [Me(1), Me(2)], ω [(H32-C31-H33), (C26-H27)] and γ [(H29-C28-H30), (H20-C8-H21), R(1), (C-O)]	-	-	-	-	288	287	297	299
τ [Me(1), Me(2)]	262	284	274	308	275	312	277	281
τ [Me(1), Me(2)], ω [R(1), R(3), (C11-C26-H27)] and γ [CH ₃ (2), (H32-C31-H33), (H29-C28-H30), (H20-C8-H21), (C-S), (N-C)]	258	255	257	256	-	-	-	-
τ [Me(1), Me(2)], ω [(H32-C31-H33), (C26-H27), (H20-C8-H21)] and γ [(H29-C28-H30), (H20-C8-H21), R(1), R(2), (O-C)]	-	-	-	-	277	277	280	275
τ [Me(2)]	-	-	-	-	261	263	262	255
ω [Me(1), (H20-C8-H21), R(1), R(3), (C11-C26-H27)] and γ [Me(2), (H32-C31-H33), (H29-C28-H30), (C-S), (N-C)]	234	235	231	236	-	-	-	-
τ [Me(2), Me(1)]	211	257	266	292	-	-	-	-
ω [Me(2), (C26-H27)] and γ [(H20-C8-H21), R(1), R(3), (H29-C28-H30)]	-	-	-	-	243	245	243	243
ω [Me(1), (H20-C8-H21), R(1), R(3)] and γ [Me(2), (H32-C31-H33), (H29-C28-H30), (C-S), (N-C)]	199	197	198	198	-	-	-	-
ω [Me(1), (H20-C8-H21), R(1), R(3)] and γ [Me(2), (H32-C31-H33), (H29-C28-H30), (O-C), (N-C)]	-	-	-	-	210	217	211	210
ω [Me(2), (C26-H27), (H29-C28-H30), (N-C)] and γ [(H20-C8-H21), R(1), R(3), Me(1), (H32-C31-H33), (C-S)]	161	163	162	164	-	-	-	-
ω [Me(2), (C26-H27), (H29-C28-H30), (N-C)] and γ [(H20-C8-H21), R(1), R(3), Me(1), (H32-C31-H33), (C-O)]	-	-	-	-	184	185	188	186
ω [Me(1), Me(2), R(3), R(1)], γ [(H32-C31-H33), (H29-C28-H30), (H20-C8-H21), (C-S)] and τ [(C-N-C-C)]	156	151	160	153	-	-	-	-

Table 2. Continued

ω [Me(1), Me(2), R(3), R(1)], γ (H32-C31-H33), (H29-C28-H30), (H20-C8-H21), (C-O)] and τ [(C-N-C-C)]	-	-	-	-	156	160	160	154
ω [(H29-C28-H30), (H32-C31-H33)], γ [R(3), Me(1), Me(2), (N-C), R(1), (H20-C8-H21), (C11-C26-H27), (C-S)]	138	134	140	140	-	-	-	-
ω [(H29-C28-H30), (H32-C31-H33)], γ [R(3), Me(1), Me(2), (N-C), R(1), (H20-C8-H21), (C11-C26-H27), (C-O)]	-	-	-	-	141	145	144	140
γ [Me(2), (H32-C31-H33), (H29-C28-H30)] and τ [(C-N-C-), Me(1), R(1), R(2), R(3)]	131	131	135	131	128	140	140	131
τ [Me(2), R(1), R(3), (C26-H27), (H32-C31-H33), (H29-C28-H30)] and γ [(H20-C8-H21), Me(1)]	94	102	100	103	105	107	101	98
τ [R(3), (C-N-C-C)], ω [Me(1), Me(2), (C11-C26-H27), (H32-C31-H33), (H29-C28-H30), (C-O)] and γ [(H20-C8-H21), R(1)]	-	-	-	-	94	94	97	93
τ [R(3), (C-N-C-C)], ω [Me(1), Me(2), (C11-C26-H27), (H32-C31-H33), (H29-C28-H30), (C-S)] and γ [(H20-C8-H21), R(1)]	83	94	87	94	-	-	-	-
τ [(C-N-C-C)] and ω [Me(1), Me(2), (H32-C31-H33 (H30-C28-H29))]	60	37	59	31	-	57	-	52
ω [Me(1), R(1), R(3), (C11-C26-H27), (H32-C31-H33), (C-O), (N-C)] and γ [Me(2), (H29-C28-H30), (H20-C8-H21)]	-	-	-	-	49	-	46	-
τ [(C-N-C-C)], γ [(R(1), R(3), (C-S), (H20-C8-H21)] and ω [Me(1), Me(2), (H32-C31-H33 (H30-C28-H29), (C11-C26-H27)]	54	44	55	45	-	-	-	-
τ [(C-N-C-C)], γ [(R(1), R(3), (C-O), (H20-C8-H21)] and ω [Me(1), Me(2), (H32-C31-H33 (H30-C28-H29), (C11-C26-H27)]	-	-	-	-	45	47	40	47
τ [(C-N-C-C)], γ [(R(1), R(3), (C-S), (H20-C8-H21), (H32-C31-H33), (H30-C28-H29)] and ω [Me(1), Me(2)]	44	52	49	53	-	-	-	-
τ [(C-N-C-C)], γ [(R(1), R(3), (C-O), (H20-C8-H21), (H32-C31-H33), (H30-C28-H29)] and ω [Me(1), Me(2)]	-	-	-	-	39	43	37	38
δ [skeleton]	20	22	28	13	21	25	33	16

v: Stretching; δ : deformation; γ : twisting; τ : torsion; ω : wagging; s: symmetric; as: asymmetric.

The ring carbon-carbon stretching vibrations occur in the region 1430-1625 cm^{-1} [15]. For the dosulepin, BLYP/PW91 calculations show that these vibrations to be 1468-1595 cm^{-1} (also 1293 cm^{-1}) and 1484-1618 cm^{-1} (also 1350, 1356 cm^{-1}) in the gas phase and 1465-1591 cm^{-1} (also 1289 cm^{-1}) and 1479-1614 cm^{-1} (also 1344, 1354 cm^{-1}) in solution media. For the doxepin, the bands at 1479-1613 cm^{-1} (also 1300 cm^{-1}) (BLYP) and 1485-1646 cm^{-1} (also 1323, 1327 cm^{-1}) (PW91) are assigned to ring carbon-carbon stretching vibrations in the gas phase and vibrations bands found at 1470-1616 cm^{-1} (also 1298 cm^{-1}) (BLYP)

and 1558-1641 cm^{-1} (also 1320, 1332 cm^{-1}) (PW91) are assigned to ring carbon-carbon stretching vibrations in solution media.

CH₂ vibrations. For the dosulepin, BLYP method assigns the wavenumbers of CH₂ stretching vibrations in R2 (H20-C8-H21) to be 2962 and 3016 cm^{-1} in the gas phase and 2972 and 3027 cm^{-1} in solution media and PW91 method assigns these wavenumbers to be 2969 and 3027 cm^{-1} in the gas phase and 2976 and 3037 cm^{-1} in solution media. For the doxepin, these vibrations were calculated 2948, 3033 cm^{-1} in the gas phase and 2969, 3046 cm^{-1} in

solution media by BLYP method and 2958, 3047 cm^{-1} in the gas phase and 2970, 3055 cm^{-1} in solution media by PW91 method.

The dosulepin CH_2 group (H32-C31-H33) asymmetric stretching vibration modes were calculated 3029, 3002 cm^{-1} (BLYP) and 3039, 3013 cm^{-1} (PW91) in the gas phase and 3031, 2998 cm^{-1} (BLYP) and 3043, 3003 cm^{-1} (PW91) in solution media. For the doxepin, these vibrations were assigned to be 2836- 3049 cm^{-1} in the gas phase and 2860-3039 cm^{-1} in solution media by BLYP method and 2853-3071 cm^{-1} in the gas phase and 2860-3057 cm^{-1} by PW91 method in solution media.

The BLYP calculations show symmetric stretching vibration modes of CH_2 group (H32-C31-H33) of dosulepin occur in 2944, 2948 cm^{-1} and 2949, 2972 cm^{-1} in the gas phase and solution media, respectively. PW91 calculations show these modes occur in 2958, 2969 cm^{-1} in the gas phase and 2952, 2976 cm^{-1} in solution media. For the doxepin, these modes have been calculated to occur at 2963 cm^{-1} (BLYP) and 2976 cm^{-1} (PW91) in the gas phase and 2964 cm^{-1} (BLYP) and 2975 cm^{-1} (PW91) in solution media.

The asymmetric stretching vibration modes of CH_2 group (H29-C28-H30) are less than CH_2 group (H32-C31-H33) modes. These modes have been calculated 3029 cm^{-1} (BLYP) and 3039 cm^{-1} (PW91) in the gas phase and 3031 cm^{-1} (BLYP) and 3043 cm^{-1} (PW91) in solution media. For the doxepin, these vibrations are assigned to occur at 3049 cm^{-1} in the gas phase and 3039 cm^{-1} in solution media by BLYP method and 3071 cm^{-1} in the gas phase and 3056 cm^{-1} in solution media by PW91 method. Symmetric stretching vibration modes for this group of dosulepin, at the B3LYP level, occur at 2944 cm^{-1} and 2949 cm^{-1} , and at the PW91 level occur at 2958 cm^{-1} and 2952 cm^{-1} in the gas phase and solution media, respectively. For the doxepin, these modes have been calculated 3025 cm^{-1} (BLYP) and 3044 cm^{-1} (PW91) in the gas phase and 3026 cm^{-1} (BLYP) and 3029 cm^{-1} (PW91) in solution media.

These results show that the ranges of calculated frequencies for the CH_2 groups of doxepin are similar to those for dosulepin in the gas phase and solution media. Also, Table 2 shows that the asymmetric and symmetric deformation modes for the dosulepin are calculated by BLYP method for the ranges 1595-1427 cm^{-1} and 1591-1410 cm^{-1} in the gas phase and by PW91 method for the

ranges 618-1415 cm^{-1} and 1614-1405 cm^{-1} in solution media. These modes were calculated by the BLYP method for the doxepin in the ranges 1613-1438 cm^{-1} and 1646-1432 cm^{-1} in the gas phase and by PW91 method for the ranges 1616-1426 cm^{-1} and 1641-1420 cm^{-1} in solution media.

C-S vibrations. The band due to C-S stretching vibrations is observed in the region 245-1035 cm^{-1} [16]. The BLYP/PW91 method shows C-S vibrations are found at 524 cm^{-1} and 529 cm^{-1} in the gas phase and at 528 cm^{-1} and 524 cm^{-1} in solution media.

C-O vibrations. The C-O stretching vibrations were calculated in the range 981-1219 cm^{-1} by BLYP method and in the range 1022-1237 cm^{-1} by PW91 method in gas phase and in the range 971-1217 cm^{-1} by BLYP method and in the range 1007-1196 cm^{-1} by PW91 method in solution media. The C-O bands occur in the region 1000-1300 cm^{-1} in literature [17].

C-N vibrations. The C-N stretching mode is reported in the range 950-1150 cm^{-1} [14, 18]. In the dosulepin, this band is assigned to be 794-1033 cm^{-1} by BLYP method and 818-1036 cm^{-1} by PW91 in gas phase and 783-1023 cm^{-1} and 809-1023 cm^{-1} in solution media. For the doxepin, C-N stretching mode is calculated in the range 820-1032 cm^{-1} and 841-1032 cm^{-1} in the gas phase and 819-1024 cm^{-1} and 834-1027 cm^{-1} in the solution media By BLYP and PW91 methods. The C-S group has less polarity than C-O and C-N groups and has considerably weaker bands. Besides the stretching vibrations, the C-O, C-S and C-N groups give rise to twisting and wagging vibrations which are listed in Table 2.

Figure 2 shows the most intense band, at BLYP-based calculation, in the infrared spectra of dosulepin occurring at 2847 cm^{-1} in symmetric stretching modes of the methyl groups (Me1, Me2), and the most intense band, at PW91-based calculation, occurring at 2873 cm^{-1} in a symmetric stretching mode of the methyl group (Me2) in the gas phase. The sharp band in the region of 2866 cm^{-1} (BLYP) and 2873 cm^{-1} (PW91) is assigned to the characteristic C-H stretching modes of the methyl groups (Me (1): (C39-H41), Me (2): (C35-H37)) in solution media. In doxepin, the C-H stretching vibrations of (C39-H41) in Me (1); (C35-H37) in Me (2) and (C31-H32), is assigned to a strong band at 2865 cm^{-1} (BLYP) and 2884 cm^{-1} (PW91) in the gas phase and 2872 cm^{-1} (BLYP) and 2894 cm^{-1} (PW91) in solution

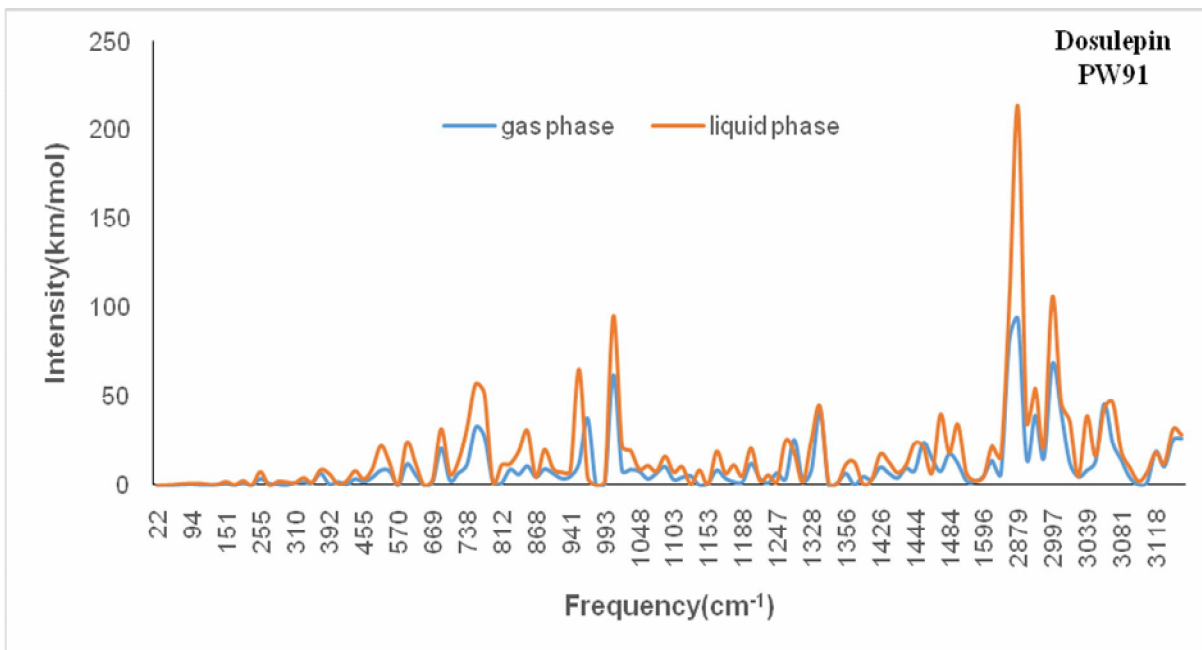
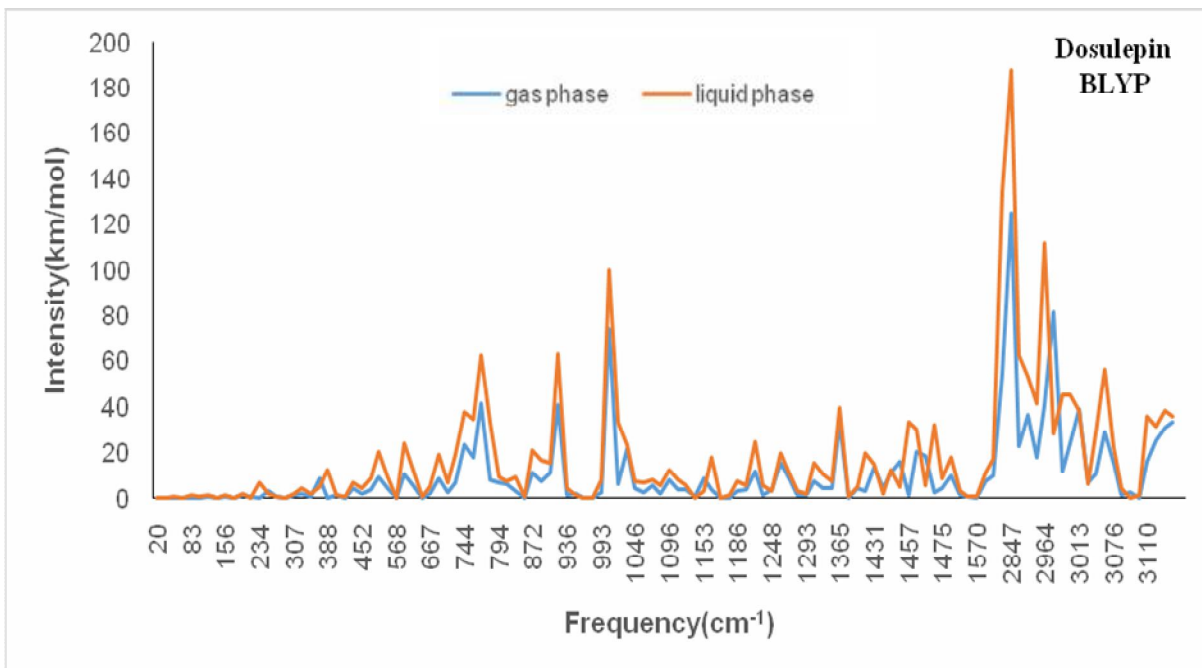


Fig. 2. IR spectra of dosulepin and doxepin in both gas and solution media (BLYP/PW91).

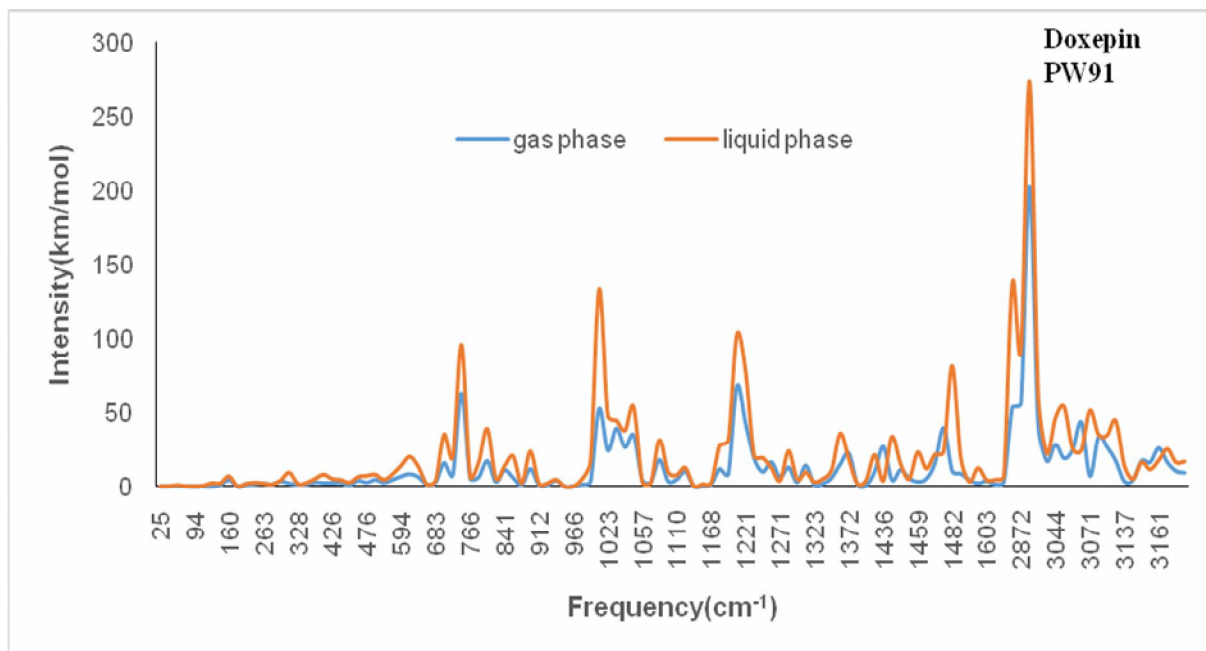
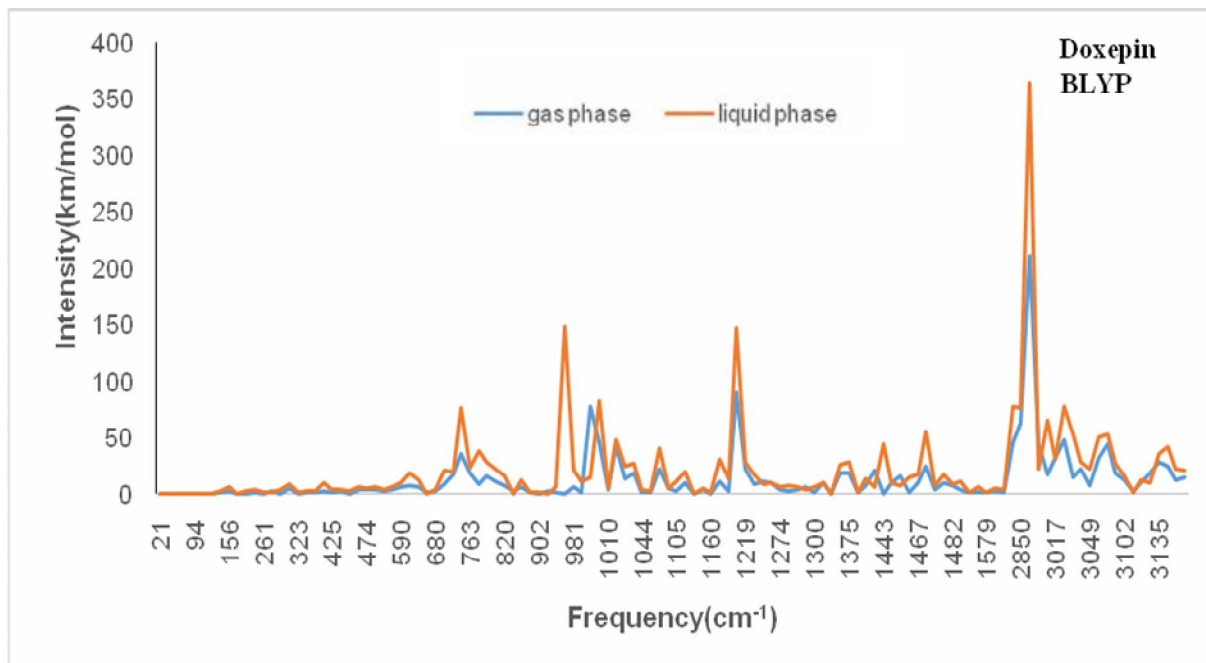


Fig. 2. Continued.

media. It may be seen from Fig. 2 that BLYP/PW91 calculations show frequencies of solution media which are larger than those of gas phase.

Calculations of Quantum Chemical Parameters

Using the optimized geometries, the energy of the highest occupied molecular orbital (E_{HOMO}), the energy of the lowest unoccupied molecular orbital (E_{LUMO}), the energy gap (ΔE), the ionization potential (IP), the electron affinity (EA), the global hardness (η), the global softness (σ), the chemical potential (χ), the dipole moment (μ) and the electrophilicity (ω) [19,20] were calculated for dosulepin and doxepin molecules (See Table 3). Table 3 shows the quantum chemical parameters of dosulepin and doxepin. These parameters give information on the chemical reactivity of the studied molecules in their gas and solution media. The trends of the quantum chemical parameters are almost similar in both gas and solution media. Also, these descriptors were calculated by both energetic and orbital modes. A higher E_{HOMO} suggests a lower capability of accepting electrons because this energy describes the electron donating ability of a molecule. The E_{LUMO} indicates the ability of a molecule to accept electrons. Thus, the lower the value of E_{LUMO} , the more probable the molecule would accept electrons. Based on quantum molecular descriptors, as given in Table 3, dosulepin has a high E_{HOMO} and a low E_{LUMO} in comparison to doxepin in both gas and solution media. The gap between the HOMO and LUMO energy levels is an important function of reactivity of a molecule. The calculations indicate that the dosulepin has a low ΔE in its gas and solution media. Thus, electron transfer from the HOMO of dosulepin to its LUMO is easier than similar electron transfer in doxepin. IP is a basic description of the chemical reactivity of atoms and molecules. High IP shows towering stability.

Table 3 shows dosulepin has a high ionization energy compared with doxepin in gas and solution media. The values of η and σ are important properties to measure the molecular stability and reactivity. Table 3 shows that dosulepin has the lowest η and the highest σ . The ability of molecules to accept electrons may be described by the ω index. It is a measure of energy stabilization of a system after the system accepts the additional amount of electron charge from its environment. Our studies indicate that

dosulepin has a high value of ω in gas and solution media.

The calculated electrodonating, electroaccepting and net electrophilicity values of dosulepin and doxepin are listed in Table 3. A larger electroaccepting value corresponds to a better capability of accepting charge, whereas a smaller value of the electrodonating value of a system makes it a better electron donor. The energy and orbital parameters indicate dosulepin molecule has a better capability of accepting charge in gas and solution media.

The polarity of a molecule describes its μ . Table 3 shows dosulepin has the highest value of μ in both gas and solution media. It is clear from Table 3 that μ values of these two drugs are higher in aqueous solution than those in the gas phase, which is an indication of the polarization effect of the solvent on the drug molecules.

The dielectric solvation energy of dosulepin is lower (-9.002 and -9.47 kcal mol⁻¹) than that of doxepin, suggesting that doxepin has a higher solubility in water than dosulepin. The high molecular mass of dosulepin causes an increase of drug adsorption onto absorbent and hence increase the efficiency uptake of the drug.

Local Molecular Reactivity

The Fukui indices permit the distinction between the reactive regions of a molecule, the nucleophilic and electrophilic behaviors of a molecule and the chemical reactivity [21]. These functions can be given by Eqs. (1) and (2) [21]:

$$f^+ = Q_{N+1} - Q_N \quad (1)$$

$$f^- = Q_N - Q_{N-1} \quad (2)$$

Q_{N+1} corresponds to an anion in which an electron is added to the LUMO of its neutral molecule. Q_{N-1} corresponds to a cation in which an electron is removed from the HOMO. Thus Q_{N+1} , Q_N and Q_{N-1} are anionic, neutral and cationic states of a material, respectively. The maximum of f^+ corresponds to a reaction with respect to nucleophilic attack and the maximum of f^- shows the preferred site for adsorption of electrophilic agents [22]. For dosulepin, the highest f^+ is associated with S atom and the highest f^- occurs at N atom in both gas and solution media. The doxepin site for nucleophilic attack is the C26 atom and for

Table 3. Quantum Chemical Descriptors of Dosulepin and Doxepin

Molecular descriptors	Parameter	Dosulepin				Doxepin			
		Gas		Solvent		Gas		Solvent	
		BLYP	PW91	BLYP	PW91	BLYP	PW91	BLYP	PW91
HOMO (eV)	-	-4.427	-4.601	-4.670	-4.852	-4.639	-4.819	-4.866	-5.048
LUMO (eV)	-	-1.606	-1.818	-1.793	-2.006	-1.442	-1.670	-1.674	-1.913
ΔE (eV)	-	2.821	2.783	2.877	2.846	3.196	3.148	3.192	3.135
IP = [E(+1) - E(0)] (eV)	Energetic	6.422	6.626	5.061	5.262	6.631	6.848	5.281	5.501
IP = -E _{HOMO} (eV)	Orbital	4.427	4.601	4.670	4.852	4.639	4.819	4.866	5.048
EA = [E(0) - E(-1)] (eV)	Energetic	-0.127	0.073	1.578	1.787	-0.367	-0.156	1.431	1.663
EA = -E _{LUMO} (eV)	Orbital	1.606	1.818	1.793	2.006	1.442	1.670	1.674	1.913
(I - A)/2 (eV) = η	Energetic	3.275	3.276	1.741	1.738	3.499	3.502	1.925	1.919
	Orbital	1.411	1.391	1.439	1.423	1.598	1.574	1.596	1.567
$\chi = (I + A)/2$ (eV)	Energetic	3.148	3.349	3.319	3.524	3.132	3.346	3.356	3.582
	Orbital	3.016	3.209	3.232	3.429	3.04	3.244	3.27	3.480
$\sigma = 1/\eta$ (eV ⁻¹)	Energetic	0.305	0.305	0.574	0.575	0.286	0.286	0.519	0.521
	Orbital	0.709	0.719	0.695	0.703	0.626	0.635	0.627	0.638
$\omega = \chi^2/2\eta$ (eV)	Energetic	1.513	1.712	3.164	3.574	1.402	1.598	2.925	3.343
	Orbital	3.225	3.701	3.63	4.133	2.892	3.344	3.35	3.865
$\omega^- = (3I + A)^2/16(I - A)$ (eV)	Energetic	3.496	3.796	5.041	5.553	3.405	3.709	4.843	5.374
	Orbital	4.91	5.480	5.425	6.025	4.612	5.163	5.184	5.801
$\omega^+ = (I + 3A)^2/16(I - A)$ (eV)	Energetic	0.348	0.447	1.722	2.029	0.273	0.363	1.487	1.792
	Orbital	1.893	2.271	2.194	2.596	1.572	1.918	1.914	2.321
$\Delta\omega_{\pm} = (\omega^+ + \omega^-)$ (eV)	Energetic	3.844	4.243	6.763	7.582	3.679	4.072	6.331	7.166
	Orbital	6.803	7.750	7.619	8.621	6.184	7.081	7.099	8.122
Dipole moment (μ) (D)	-	1.573	1.575	2.542	2.507	0.949	0.937	1.585	1.558
Solvation energy (kcal mol ⁻¹)	-	-	-	-9.002	-9.47	-	-	-9.852	-10.39

Table 4. Calculated Fukui Functions for Electrophilic Agents

Atom	Dosulepin				Doxepin			
	Gas		Solvent		Gas		Solvent	
	BLYP	PW91	BLYP	PW91	BLYP	PW91	BLYP	PW91
C1	0.036	0.037	0.049	0.049	0.034	0.036	0.047	0.046
C2	0.038	0.040	0.054	0.053	0.013	0.013	0.022	0.021
C3	-0.003	0.000	0.014	0.012	0.006	0.007	0.024	0.026
C4	0.028	0.024	0.026	0.028	0.004	0.003	0.016	0.018
C5	0.024	0.024	0.034	0.028	0.016	0.017	0.028	0.030
C6	0.004	0.005	0.019	0.019	0.010	0.009	0.017	0.018
O	-	-	-	-	0.015	0.013	0.012	0.013
S	0.099	0.094	0.094	0.092	-	-	-	-
C8	-0.014	-0.012	-0.006	-0.003	-0.017	-0.016	-0.008	-0.007
C9	0.011	0.014	0.030	0.030	0.024	0.025	0.035	0.038
C10	0.025	0.023	0.041	0.042	0.034	0.034	0.041	0.042
C11	-0.003	0.002	0.005	0.008	0.020	0.024	0.032	0.032
C12	0.009	0.010	0.022	0.026	0.022	0.023	0.038	0.040
C13	0.015	0.016	0.023	0.023	0.011	0.011	0.024	0.027
C14	0.041	0.045	0.056	0.059	0.061	0.063	0.076	0.075
C15	0.004	0.005	0.014	0.017	0.012	0.014	0.026	0.028
C26	0.077	0.074	0.082	0.092	0.098	0.103	0.121	0.120
C28	-0.028	-0.021	-0.022	-0.019	-0.029	-0.030	-0.027	-0.027
C31	-0.005	-0.005	0.003	-0.005	-0.003	-0.002	-0.005	-0.005
N34	0.013	0.010	0.000	0.007	-0.007	-0.007	0.000	0.000
C35	-0.009	-0.009	0.006	-0.005	-0.014	-0.014	-0.003	-0.003
C39	-0.012	-0.015	-0.005	-0.004	-0.014	-0.013	-0.004	-0.004

electrophilic attack is the N atom in both gas and solution media. The calculated values of the Fukui functions are reported in Tables 4 and 5.

Thermodynamic Properties

Thermodynamic properties are used to describe the effects of temperature on structural stabilities of materials.

Entropy (S), heat capacity (C_p), enthalpy (H) and Gibbs free energy (G) of dosulepin and doxepin were calculated at different temperatures in both gas and solution media. The results show that the evaluated thermodynamic data for two compounds are very similar and near together. Since they have similar structures and the difference is the presence of oxygen (in the doxepin) and sulfur (in the dosulepin).

Table 5. Calculated Fukui Functions for Nucleophilic Agents

Atom	Dosulepin				Doxepin			
	Gas		Solvent		Gas		Solvent	
	BLYP	PW91	BLYP	PW91	BLYP	PW91	BLYP	PW91
C1	0.002	0.004	0.006	0.006	0.008	0.009	0.004	0.006
C2	0.000	0.000	0.005	0.005	0.004	0.004	0.001	0.003
C3	-0.006	-0.009	0.001	0.002	0.002	0.001	0.002	0.004
C4	-0.017	-0.015	-0.005	-0.011	-0.012	-0.013	-0.001	-0.002
C5	-0.007	-0.008	0.002	0.001	0.002	0.001	0.006	0.004
C6	0.000	0.000	0.005	0.006	0.005	0.005	0.001	0.004
O	-	-	-	-	-0.003	-0.001	0.002	0.002
S	0.022	0.022	0.021	0.021	-	-	-	-
C8	-0.005	-0.005	0.000	-0.003	-0.006	-0.006	0.000	-0.001
C9	0.007	0.006	0.006	0.007	0.005	0.005	0.007	0.006
C10	-0.009	-0.007	-0.001	0.000	-0.012	-0.013	0.001	0.000
C11	0.049	0.050	0.030	0.034	0.039	0.040	0.015	0.019
C12	0.001	0.002	0.007	0.006	-0.008	-0.008	0.000	0.000
C13	0.004	0.006	0.005	0.006	0.002	0.002	0.003	0.003
C14	0.013	0.014	0.009	0.011	0.009	0.010	0.004	0.007
C15	0.003	0.004	0.005	0.005	0.005	0.005	0.002	0.004
C26	-0.028	-0.020	0.009	0.007	-0.024	-0.026	-0.001	0.002
C28	-0.003	-0.009	-0.006	-0.003	-0.023	-0.022	-0.020	-0.021
C31	-0.035	-0.033	-0.027	-0.020	-0.057	-0.057	-0.042	-0.039
N34	0.166	0.167	0.223	0.212	0.197	0.198	0.250	0.238
C35	-0.048	-0.045	-0.037	-0.028	-0.054	-0.052	-0.029	-0.028
C39	-0.053	-0.046	-0.026	-0.024	-0.056	-0.054	-0.030	-0.028

Nevertheless, in order to evaluate the effect of these atoms in dosulepin and doxepin, their thermodynamic properties are studied.

The corresponding fitting equations used to calculate thermodynamic properties of dosulepin and doxepin are shown in Table 6. These equations could be used for interaction of dosulepin or doxepin with other compounds.

For example, in order to calculate the Gibbs free energy of the reaction of dosulepin with any other compounds, thermodynamic properties of dosulepin could be obtained from these equations, which will in turn help to judge the spontaneity of the reaction.

It can be seen from Figure 3 and Table 6 that the Gibbs free energy gradually decreases with the increase in

Table 6. Equations Used to Calculate Thermodynamic Properties of Dosulepin and Doxepin in Gas and Liquid Phases (BLYP and PW91)

Compound	Phase	B3LYp	PW91	R ²
Dosulepin	Gas	$S = 57.8624 + 0.3152T - 6.5 \times 10^{-5}T^2$	$S = 58.2878 + 0.3131T - 6.4 \times 10^{-5}T^2$	$R^2 = 0.9998$
		$C_p = 1.8980 + 0.3043T - 12 \times 10^{-5}T^2$	$C_p = 1.7609 + 0.3035T - 12 \times 10^{-5}T^2$	$R^2 = 0.9991$
		$H = 213.2359 + 0.0261T - 9.22 \times 10^{-5}T^2$	$H = 214.1885 + 0.0257T - 9.23 \times 10^{-5}T^2$	$R^2 = 0.9994$
	Solution	$H = 214.1885 + 0.0257T - 9.23 \times 10^{-5}T^2$	$H = 214.1885 + 0.0257T - 9.23 \times 10^{-5}T^2$	$R^2 = 0.9999$
		$S = 56.8021 + 0.3133T - 6.4 \times 10^{-5}T^2$	$S = 59.3958 + 0.3122T - 6.3 \times 10^{-5}T^2$	$R^2 = 0.9998$
		$C_p = 1.2679 + 0.3069T - 12 \times 10^{-5}T^2$	$C_p = 1.4947 + 0.3047T - 12 \times 10^{-5}T^2$	$R^2 = 0.9991$
		$H = 213.0843 + 0.0259T - 9.25 \times 10^{-5}T^2$	$H = 213.9557 + 0.0259T - 9.25 \times 10^{-5}T^2$	$R^2 = 0.9994$
		$G = 216.6616 - 0.0706T - 12 \times 10^{-5}T^2$	$G = 217.4961 - 0.0732T - 12 \times 10^{-5}T^2$	$R^2 = 0.9999$
Doxepin	Gas	$S = 58.43 + 0.3049T - 6.0 \times 10^{-5}T^2$	$S = 57.4308 + 0.3017T - 5.8 \times 10^{-5}T^2$	$R^2 = 0.9999$
		$C_p = 1.1794 + 0.2997T - 11 \times 10^{-5}T^2$	$C_p = 0.7358 + 0.2994T - 11 \times 10^{-5}T^2$	$R^2 = 0.9987$
		$H = 216.1582 + 0.0240T - 9.27 \times 10^{-5}T^2$	$H = 217.6176 + 0.0235T - 9.28 \times 10^{-5}T^2$	$R^2 = 0.9995$
	Solution	$G = 219.4815 - 0.0714T - 12 \times 10^{-5}T^2$	$G = 220.8698 - 0.0699T - 12 \times 10^{-5}T^2$	$R^2 = 0.9999$
		$S = 57.8009 + 0.3042T - 5.9 \times 10^{-5}T^2$	$S = 58.8421 + 0.3049T - 6 \times 10^{-5}T^2$	$R^2 = 0.9999$
		$C_p = 0.8599 + 0.30122T - 12 \times 10^{-5}T^2$	$C_p = 1.1337 + 0.3000T - 12 \times 10^{-5}T^2$	$R^2 = 0.9987$
		$H = 216.0178 + 0.0239T - 9.29 \times 10^{-5}T^2$	$H = 216.8479 + 0.0224T - 9.27 \times 10^{-5}T^2$	$R^2 = 0.9995$
		$G = 219.3296 - 0.0705T - 12 \times 10^{-5}T^2$	$G = 220.1785 - 0.0718T - 12 \times 10^{-5}T^2$	$R^2 = 0.9999$

temperature, while entropy, heat capacity and enthalpy gradually increase with temperature in both gas and solution media. The smaller Gibbs free energy is indicative of the better thermal stability of the compound [23]. Figure 4 and Table 6 show that thermal stability of dosulepin is slightly better than doxepin in both gas and solution media.

CONCLUSIONS

Theoretical studies of the vibrational spectra, molecular

structure and thermodynamic properties of dosulepin and doxepin were carried out in gas and solution media by GGA-BLYP and GGA-PW91 modeling methods. Computational and chemical simulations were carried out for these drugs. Quantum chemical parameters of dosulepin and doxepin were calculated and compared. The simulation results show that dosulepin is quite a reactive drug. Values have been assigned to the vibrational frequencies of the fundamental modes of these compounds. The BLYP/PW91 analyses of the wavenumbers show that the frequencies assigned to doxepin are higher than those assigned to

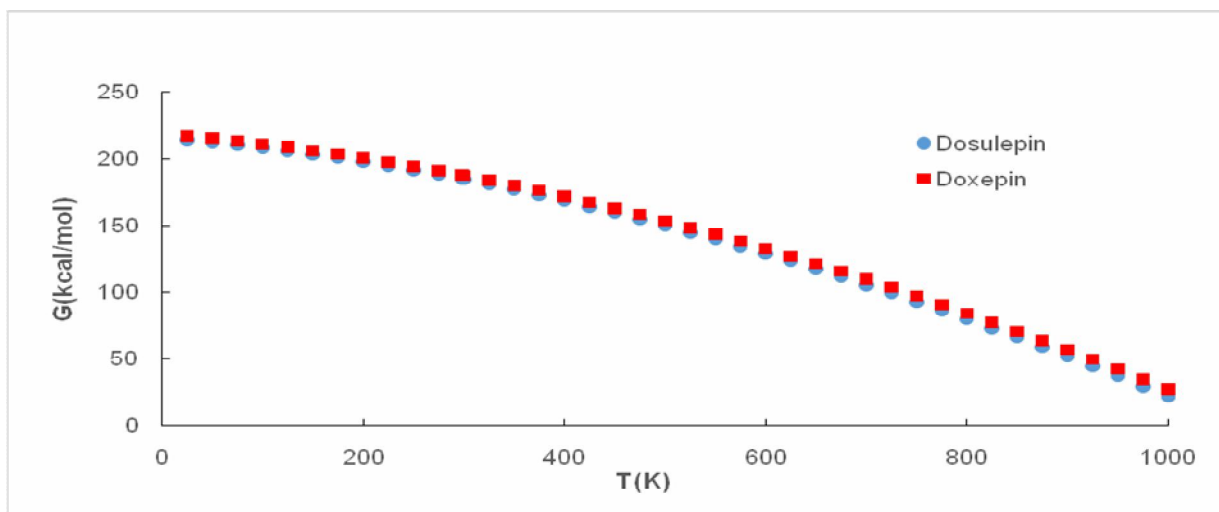


Fig. 3. Thermodynamic properties of dosulepin calculated by BLYP at different temperatures in gas phase.

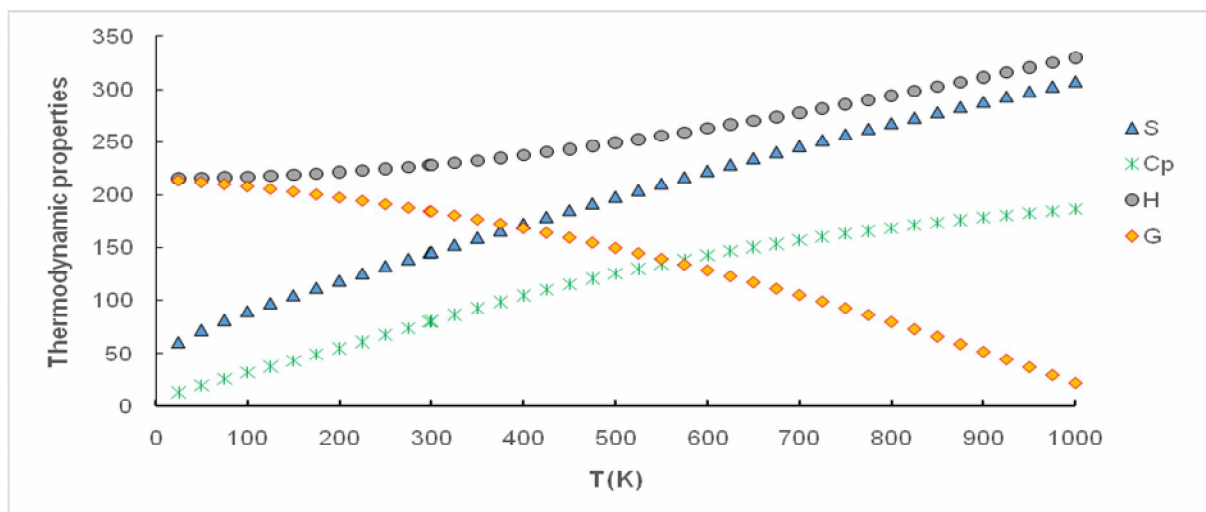


Fig. 4. The Gibbs free energies of dosulepin and doxepin as a function of temperature in gas phase (BLYP).

dosulepin in gas and solution media

The bond length of C-O is shorter than that of C-S. The shorter bond length of C-O is responsible for the appearance of the high frequency peaks in compounds infrared spectra. The Fukui index results show that the site for electrophilic attack is an N atom in dosulepin and doxepin molecules.

The thermodynamic properties of dosulepin and doxepin were calculated at different temperatures and the correlations between entropy, heat capacity, enthalpy, Gibbs free energy and temperatures have also been determined for these compounds. Dosulepin and doxepin can be attractive drugs for further medicinal and pharmacological studies.

ACKNOWLEDGEMENTS

This work was supported by Graduate University of Advanced Technology and Research Center for Science, High Technology & Environmental Science, Kerman. This article was peer reviewed by Nasser Mirzai Baghini, Imperial College Reactor Centre, Silwood Park, Ascot, Berkshire, United Kingdom.

REFERENCES

- [1] Stolerman, I. P.: *Encyclopedia of psychopharmacology*; Springer Science & Business Media, 2010, Vol. 2.
- [2] Jalander, L.; Oksanen, L.; ähtinen, J. Synthesis of dothiepin and doxepin by grignard reactions in toluene. *Synthetic Commun.*, **1989**, *19*, 3349-3352, DOI: 10.1080/00397918908052739.
- [3] Abdellatef, H. E.; El-Henawee, M. M.; El-Sayed, H. M.; Ayad, M. M. Spectrophotometric and spectrofluorimetric methods for analysis of tramadol, acebutolol and dothiepin in pharmaceutical preparations. *Spectrochim. Acta A: Mol. Biomol. Spectroscopy*, **2006**, *65*, 1087-1092, DOI: 0.1016/j.saa.2006.02.008.
- [4] Sankaranarayanan, R.; Siva, S.; Venkatesh, G.; Prabhu, A. A. M.; Rajendiran, N. Dual fluorescence of dothiepin, doxepin drugs-effect of solvents and β -cyclodextrin. *J. Mol. Liq.*, **2011**, *161*, 107-114, DOI: 10.1016/j.molliq.2011.04.016.
- [5] More details about DMol³ can be found at <http://www.accelrys.com/mstudio/DMol3.html>.
- [6] Delley, B. An all-electron numerical method for solving the local density functional for polyatomic molecules. *J. Chem. phys.*, **1990**, *92*, 508-517, DOI:10.1063/1.458452.
- [7] Delley, B. Fast calculation of electrostatics in crystals and large molecules. *J. Phys. Chem.*, **1996**, *100*, 6107-6110, DOI: 10.1021/jp952713n.
- [8] Becke, A. D., A multicenter numerical integration scheme for polyatomic molecules. *J. Chem. phys.*, **1988**, *88*, 2547-2553, DOI: 10.1063/1.454033.
- [9] Becke, A. D., Density-functional thermochemistry. III. The role of exact exchange. *J. Chem. phys.*, **1993**, *98*, 5648-5652, DOI: 10.1063/1.464913.
- [10] Perdew, J. P.; Wang, Y. Accurate and simple analytic representation of the electron-gas correlation energy. *Phys. Rev. B*, **1992**, *45*, 13244, DOI: 10.1103/PhysRevB.45.13244.
- [11] Lee, C.; Yang, W.; Parr, R. G. Development of the Colle-Salvetti correlation-energy formula into a functional of the electron density. *Phys. Rev. B*, **1988**, *37*, 785-789; DOI: 10.1103/PhysRevB.37.785.
- [12] Andzelm, J.; Kölmel, C.; Klamt, A. Incorporation of solvent effects into density functional calculations of molecular energies and geometries. *J. Chem. Phys.*, **1995**, *103*, 9312-9320, DOI: 10.1063/1.469990.
- [13] Shigeru, O., *Organic Sulfur Chemistry: Structure and Mechanism*. London: CRC Press, 1991.
- [14] Roeges, N. P., *A guide to the complete interpretation of infrared spectra of organic structures*; Wiley, 1994.
- [15] Varsányi, G., *Assignments for vibrational spectra of seven hundred benzene derivatives*; Halsted Press, 1974, Vol. 1.
- [16] George, S., *Infrared and Raman Characteristic Group Frequencies-Tables and Charts*. Wiley, Chichester, **2001**.
- [17] Silverstein, R. M.; Webster, F. X.; Kiemle, D.; Bryce, D. L., *Spectrometric identification of organic compounds*; John Wiley & Sons, 2014.
- [18] Kundoo, S.; Banerjee, A.; Saha, P.; Chattopadhyay, K. Synthesis of crystalline carbon nitride thin films by electrolysis of methanol-urea solution. *Mater. Lett.* **2003**, *57*, 2193-2197, DOI: 10.1016/S0167-577X(02)01172-2.
- [19] Chattaraj, P. K.; Sarkar, U.; Roy, D. R., Electrophilicity index. *Chem. Rev.* **2006**, *106*, 2065-2091, DOI: 10.1021/cr040109f.
- [20] Hazarika, K. K.; Baruah, N. C.; Deka, R. C., Molecular structure and reactivity of antituberculosis drug molecules isoniazid, pyrazinamide, and 2-methylheptylisonicotinate: a density functional approach. *Struct. Chem.*, **2009**, *20*, 1079-1085, DOI: 10.1007/s11224-009-9512-2.
- [21] Gece, G.; Bilgiç, S., A theoretical study on the inhibition efficiencies of some amino acids as corrosion inhibitors of nickel. *Corros. Sci.*, **2010**, *52*,

- 3435-3443, DOI: 10.1016/j.corsci.2010.06.015
- [22] Yang, W.; Mortier, W. J., The use of global and local molecular parameters for the analysis of the gas-phase basicity of amines. *J. Am. Chem. Soc.*, **1986**, *108*, 5708-5711, DOI: 10.1021/ja00279a008.
- [23] Anderson, O. L., A simplified method for calculating the Debye temperature from elastic constants. *J. Phys. Chem. Solids*, **1963**, *24*, 909-917, DOI: 10.1016/0022-3697(63)90067-2.